International Journal of
Molecular Sciences

MDPI

Article

The Plant Derived 3-3′-Diindolylmethane (DIM) Behaves as CB_2 Receptor Agonist in Prostate Cancer Cellular Models

Paolo Tucci [1,*], Iain Brown [2], Guy S. Bewick [3], Roger G. Pertwee [3] and Pietro Marini [4]

[1] Department of Clinical and Experimental Medicine, University of Foggia, 71122 Foggia, Italy
[2] Division of Applied Medicine, School of Medicine and Dentistry, Foresterhill, University of Aberdeen, Aberdeen AB25 2ZD, UK
[3] The Institute of Medical Sciences, Foresterhill, University of Aberdeen, Aberdeen AB25 2ZD, UK
[4] Institute of Education in Healthcare and Medical Sciences, Foresterhill, University of Aberdeen, Aberdeen AB25 2ZD, UK
* Correspondence: paolo.tucci@unifg.it

Abstract: 3-3′-Diindolylmethane (DIM) is a biologically active dimer derived from the endogenous conversion of indole-3-carbinol (I3C), a naturally occurring glucosinolate found in many cruciferous vegetables (i.e., *Brassicaceae*). DIM was the first pure androgen receptor antagonist isolated from the *Brassicaceae* family and has been recently investigated for its potential pharmacological use in prostate cancer prevention and treatment. Interestingly, there is evidence that DIM can also interact with cannabinoid receptors. In this context, by considering the well-known involvement of the endocannabinoid system in prostate cancer, we have pharmacologically characterized the properties of DIM on both CB_1 and CB_2 cannabinoid receptors in two human prostate cancer cell lines: PC3 (androgen-independent/androgen receptor negative) and LNCaP (androgen-dependent). In the PC3 cell line, DIM was able to activate CB_2 receptors and potentially associated apoptotic pathways. On the other hand, although DIM was also able to activate CB_2 receptors in the LNCaP cell line, no apoptotic effects were observed. Our evidence confirms that DIM is a CB_2 receptor ligand and, moreover, it has a potential anti-proliferative effect on androgen-independent/androgen receptor-negative prostate cancer cells.

Keywords: DIM; CB_2 cannabinoid receptors; prostate cancer

Citation: Tucci, P.; Brown, I.; Bewick, G.S.; Pertwee, R.G.; Marini, P. The Plant Derived 3-3′-Diindolylmethane (DIM) Behaves as CB_2 Receptor Agonist in Prostate Cancer Cellular Models. *Int. J. Mol. Sci.* **2023**, *24*, 3620. https://doi.org/10.3390/ijms24043620

Academic Editors: Thomas Efferth, Michele Navarra, Santa Cirmi and Alessandro Maugeri

Received: 28 November 2022
Revised: 30 January 2023
Accepted: 9 February 2023
Published: 11 February 2023

1. Introduction

3-3′-Diindolylmethane (DIM) is a biologically active dimer derived from the conversion of indole-3-carbinol (I3C). I3C is produced endogenously from naturally occurring glucosinolates (GLs) contained in a wide variety of plant food substances, including members of the family *Cruciferae*, and particularly members of genus *Brassica* [1–3]. The amount of GLs in *Brassicaceae* vegetables is 206–3895 mg/kg [4]. Whether the plant tissues are crushed or cooked, an endogenous thioglucosidase (myrosinase) is activated and converts glucosinolates to indoles, principally to I3C [5]. When I3C is orally ingested, due to its chemical instability in acidic conditions, such as in the stomach environment, the compound is promptly condensed into DIM, which is the bioactive product [6], as demonstrated by pharmacokinetics studies conducted in animals [7,8] and human models [9,10]. DIM has been shown to possess hepatoprotective, antioxidant and anticancer properties [11–13]. In particular, the anticancer effect of DIM has been positively associated with a reduction of cancer incidence when a regular consumption of cruciferous vegetables is part of the dietary regime [14]. Specifically, DIM can induce apoptosis and can reduce proliferation and metastasis of tumor cells, as well as the inflammation process. Moreover, DIM appears to be a promising agent for the prevention of the recurrence of hormone-dependent cancers, such as prostate cancer [6]. In this context, hormone-dependent prostate cancer represents the sixth leading cause of cancer deaths in males, as well as the second most common

form [15]. Indeed, most prostate cancer cases are dependent on androgen at initial stages, and the inhibition of the function of androgen receptors (AR) (i.e., by using anti-androgen drugs), is currently a coadjutant therapeutical approach, along with surgery or radiation, in the treatment of this type of cancer [16]. Moreover, DIM is the first androgen receptor antagonist derived from plants with a binding affinity similar to antiandrogens, such as cyproterone acetate and bicalutamide. In addition, it can downregulate AR signaling to prevent the translocation of these receptors from the cytoplasm to the nucleus [17]. Interestingly, DIM has also demonstrated an ability to antagonize the aryl hydrocarbon receptor [18], as well as modulate cytochrome P450 1A1 activity [19]. Further evidence has also confirmed the protective role of DIM in androgen-independent prostate cancer. For example, microarray analysis conducted on PC3 cells (androgen-independent/androgen receptor negative) showed that many genes involved in the control of carcinogenesis and cell survival are modulated in their expression by indoles, including DIM [20]. Similarly, clinical trial results have demonstrated the therapeutic efficacy of DIM in the treatment of patients with high-grade prostatic intraepithelial neoplasia [21]. DIM has been demonstrated to interact with the endocannabinoid system, by stimulating both CB_1 and CB_2 cannabinoid receptors. Specifically, in an experimental model using hCB_1/CB_2-CHO transfected cells, DIM was able to interact as a slight inverse agonist on CB_1 receptors and as a partial agonist on CB_2 receptors [22]. Therefore, the endocannabinoid system has been proposed as a possible target for the treatment of prostate cancer, and extensive studies have demonstrated the involvement of the system in the pathology. In fact, results from preclinical studies have highlighted altered levels of endocannabinoids in patients' plasma and identified a correlation between high CB_1/CB_2 receptor expression and a poor prognosis [23,24]. In human prostate cancer cell lines (e.g., LNCaP and PC3), higher levels of CB_1 and CB_2 receptor expressions are detected in comparison with non-cancerous prostate cells [25], plus elevated levels for the enzymes responsible for endocannabinoid degradation, suggesting a potential role of the endocannabinoid system in prostate cell proliferation [26]. In fact, a number of synthetic and endogenous agonist ligands for CB_1 and CB_2 receptors, along with inhibitors of endocannabinoid enzyme degradation, have anticancer effects [27]. In PC3 cells and in primary cultures from benign prostate hyperplasia or prostate cancer, the endocannabinoid system is responsible for decreasing cell viability, mostly through the activation of CB_1 receptors [28]. Considering the role played by the endocannabinoid system in prostate cancer, and the potential anticancer effect of DIM, the aim of this study was to characterize the ability of DIM to interact with both CB_1 and CB_2 receptors and to evaluate any effect on apoptotic processes in cellular models of prostate cancer, such as PC3 (androgen-independent human prostate cancer cells) and LNCaP (androgen-dependent human prostate cancer cell line) that naturally express the endocannabinoid system [29,30].

2. Results

2.1. DIM Is a CB_2 Receptor Agonist in Both PC3 and LNCaP Cells

When tested in PC3 cell membranes, DIM was able to stimulate [^{35}S]GTPγS binding (EC_{50}: 9.28 nM) showing full agonist behavior (Figure 1a) with a potency similar to that of the full CB_1/CB_2 receptor agonist CP 55,940 (EC_{50}: 6.14 nM) (Figure 1d). To determine whether the elicited effect of DIM was due to the activation of CB_1 or CB_2 receptors, we tested whether the effect of DIM could be antagonized with well-known CB_1 and CB_2 receptor antagonists/inverse agonists SR141716A (SR1) and SR144528 (SR2) respectively. SR1 (10 nM) produced no significant dextral shift in the log concentration–response curve (Figure 1b). Conversely, SR2 (10 nM) did produce a significant dextral shift in the log concentration–response curve of DIM (Figure 1c). As a positive control, the effect of CP 55,940 was assayed in the same system producing a marked dextral shift in the log concentration–response dose observed in the presence of SR2 (10 nM) in addition to a slight, but significant, dextral shift in the log concentration–response in the presence of SR1 (10 nM) (Figure 1e,f, respectively).

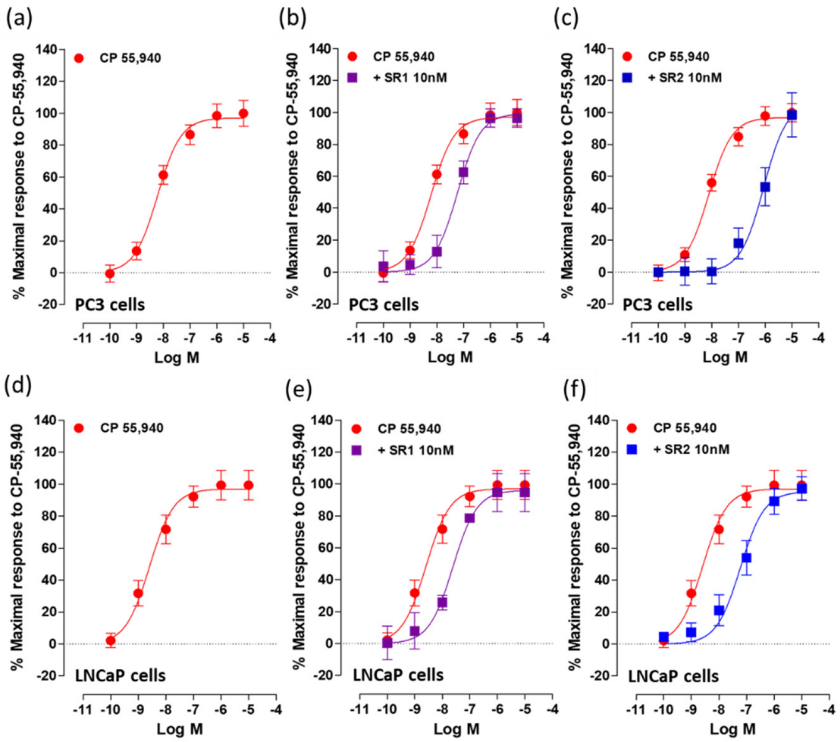

Compound	CP 55,940 (CP)	+ SR141716A (SR1), 10nM	+ SR144528 (SR2), 10nM
EC_{50} (nM)	6.14	59.35	880.70
EC_{50} 95% C.I. (nM)	3.65 – 10.33	30.31 – 116.20	329.00 - 2396
pEC_{50}	8.211	7.227	6.052
pEC_{50} 95% C.I.	8.437 – 7.986	7.518 – 6.935	6.483 – 5.620
E_{max}	97.00	99.32	106.20
E_{max} 95% C.I.	89.05 – 104.9	86.56 – 112.10	78.89 – 133.50

Compound	CP 55,940 (CP)	+ SR141716A (SR1), 10nM	+ SR144528 (SR2), 10nM
EC_{50} (nM)	2.56	59.35	59.79
EC_{50} 95% C.I. (nM)	1.31 – 50.26	30.31 – 116.20	329.00 - 2396
pEC_{50}	8.591	7.227	7.223
pEC_{50} 95% C.I.	8.884 – 8.299	7.518 – 6.935	7.564 – 6.882
E_{max}	96.98	99.32	95.39
E_{max} 95% C.I.	88.00 – 106.0	86.56 – 112.10	82.51 – 108.30

Figure 1. Effects of DIM and CP 55,940 on [^{35}S]GTPγS in PC3 cell membranes. The effects of CP 55,940 and DIM (**a**,**d** respectively) were also tested in the presence of CB_1 receptor antagonist SR1 (**b**,**e**) and CB_2 receptor antagonist SR2 (**c**,**f**). Each data point is the mean percentage value ± S.E.M. (n = 15). EC_{50}, E_{max} and pEC_{50} values and 95% confidence intervals are shown in the table.

In LNCaP cell membranes, DIM was able to stimulate [^{35}S]GTPγS binding (EC_{50}: 32.06 nM) with less potency compared to CP 55,940 (EC_{50}: 2.56 nM) (Figure 2a,d). As shown in Figure 2c, in the presence of the CB_2 receptor antagonist SR2 (10 nM), a significant dextral shift in the log concentration–response curve of DIM was observed, whilst no significant effect was observed in presence of the CB_1 receptor antagonist SR1 (Figure 2b). Since there was no evidence of a significant interaction of DIM with CB_1 receptors, further experiments with intact cells focused on its actions through CB_2 receptors.

2.2. DIM Induces an Antiproliferative Effect through CB_2 Receptor Stimulation Only in PC3 Cells

When tested in the cell viability assay, DIM was able to induce an antiproliferative effect in PC3 cells (IC_{50}: 38.93 μM) (Figure 3a). This apoptotic effect was antagonized by the CB_2 receptor antagonist SR2, with a significant dextral shift in the log concentration–response observed. Interestingly, while DIM also induced an antiproliferative effect in LNCaP cells, no antagonist effect with SR2 was observed (Figure 3b), indicating this was not via CB_2 receptors, so these were not considered further. To better understand the CB_2-mediated effects, further experiments were conducted on PC3 cells.

In PC3 cells, DIM was able to inhibit FSK-induced cAMP production with a potency in the nanomolar range (IC_{50}: 13.49 nM) (Figure 4b), showing a similar effect to the well-known CB_1/CB_2 receptor agonist CP 55,940 (IC_{50}: 4.85 nM) (Figure 4a). The inhibitory effect of both DIM and CP 55, 940 on FSK-induced cAMP production, was tested in presence of the CB_2 receptor antagonist SR2. Again, as for the viability assay, when tested at the dose of 10 nM, SR2 did not induce any significant effect on FSK-induced cAMP production inhibition elicited in the presence of both CP 55,940 and DIM. However, previous studies suggest a dextral shift requires a much higher dose of antagonists in an intact cell assay compared to isolated cell membranes [31–33]. At the dose of 100 nM, SR2 was indeed able to significantly inhibit both CP 55,940 and DIM effects on FSK-induced cAMP production

(Figure 4a,b). In contrast, the CB_1 receptor antagonist SR1 had no effect on DIM's inhibition of FSK-induced cAMP production.

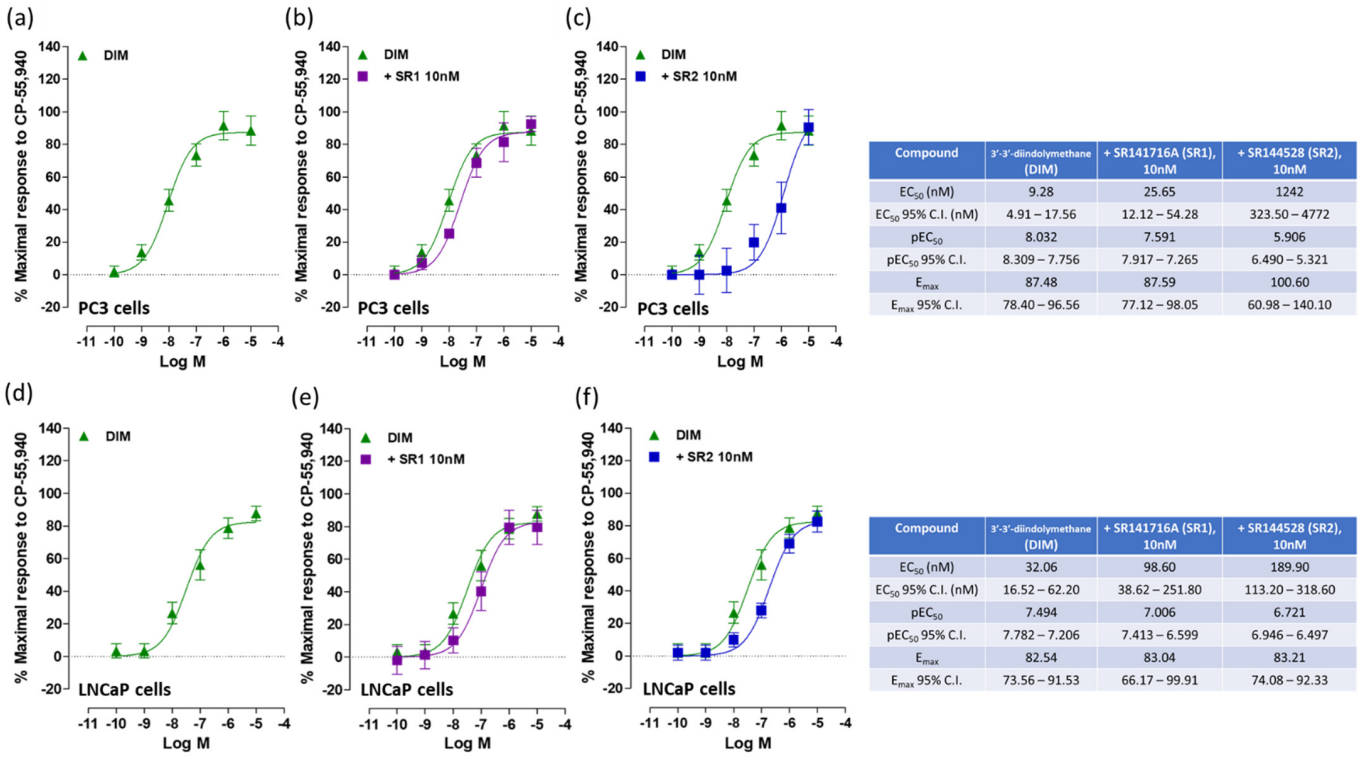

Compound	3'-3'-diindolylmethane (DIM)	+ SR141716A (SR1), 10nM	+ SR144528 (SR2), 10nM
EC_{50} (nM)	9.28	25.65	1242
EC_{50} 95% C.I. (nM)	4.91 – 17.56	12.12 – 54.28	323.50 – 4772
pEC_{50}	8.032	7.591	5.906
pEC_{50} 95% C.I.	8.309 – 7.756	7.917 – 7.265	6.490 – 5.321
E_{max}	87.48	87.59	100.60
E_{max} 95% C.I.	78.40 – 96.56	77.12 – 98.05	60.98 – 140.10

Compound	3'-3'-diindolylmethane (DIM)	+ SR141716A (SR1), 10nM	+ SR144528 (SR2), 10nM
EC_{50} (nM)	32.06	98.60	189.90
EC_{50} 95% C.I. (nM)	16.52 – 62.20	38.62 – 251.80	113.20 – 318.60
pEC_{50}	7.494	7.006	6.721
pEC_{50} 95% C.I.	7.782 – 7.206	7.413 – 6.599	6.946 – 6.497
E_{max}	82.54	83.04	83.21
E_{max} 95% C.I.	73.56 – 91.53	66.17 – 99.91	74.08 – 92.33

Figure 2. Effects of DIM and CP 55,940 on [^{35}S]GTPγS in LNCaP cell membranes. The effects of DIM and CP 55,940 (**a**,**d** respectively) were also tested in the presence of CB_1 receptor antagonist SR1 (**b**,**e**) and CB_2 receptor antagonist SR2 (**c**,**f**). Each data point is the mean percentage value ± S.E.M. (n = 15). EC_{50}, E_{max}, pEC_{50} and 95% confidence intervals are shown in the table.

2.3. DIM Induces Changes in pAKT (Reduction) and Cleaved-CASP-3 (Increase) Levels through CB_2 Receptor Stimulation in PC3 Cell Line

Since DIM had an antiproliferative effect on PC3 cells, we tested the compound for its ability to modulate the expression of the phosphorylated form of AKT (pAKT) at doses of 50 nM and 50 µM. There was no significant reduction at 50 nM but at the higher dose of 50 µM, a strong and significant reduction of pAKT level was observed (Figure 5, lanes 2 and 3). To further determine if the effect of DIM on pAKT was CB_2 receptor-mediated, two different doses (10 nM and 100 nM) of the CB_2 receptor antagonist SR2 were tested. At 10 nM, SR2 also had no significant effect when applied with the ineffective dose of DIM (50 nM; Figure 5, lane 4). However, 100 nM SR2 actually caused a strong increase of pAKT level in the presence of 50 nM DIM (Figure 5, lane 5), indicating a strong inverse agonism effect.

The robust reduction of the pAKT level produced by 50 µM DIM (Figure 5, lane 3) was only marginally, but significantly, reduced by low dose SR2 (Figure 5, lane 6 vs. lane 3), whereas at the higher dose of 100 nM, the CB_2 receptor antagonist essentially reversed the DIM-induced pAKT level decrease (Figure 5, lane 7).

Given this evidence for the regulation of pAKT levels in PC3 cells, the same experimental protocol described above was used to test the ability of DIM to modulate the activity of CASP-3. Both doses of DIM, 50 nM and 50 µM, induced a significant increase of cleaved CASP-3 level in PC3 cells (Figure 6, lanes 2 and 3) and this increase was antagonized by SR2 in a dose-related manner (Figure 6, lanes 4–7).

(a)

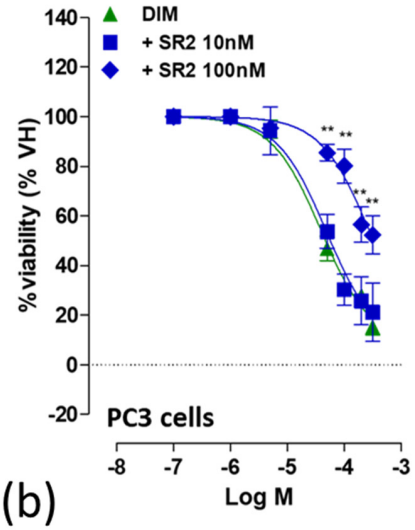

Compound	3′-3′-diindolymethane (DIM)	+ SR144528 (SR2), 10nM	+ SR144528 (SR2), 100nM
IC_{50} (μM)	38.93	47.77	286.5
IC_{50} 95% C.I. (μM)	25.65 – 59.07	15.61 – 152.3	68.22 – 1203
pIC_{50}	4.410	4.312	3.543
pIC_{50} 95% C.I.	4.491 – 4.229	4.807 – 3.817	4.166 – 2.920
I_{max}	8.50	7.32	6.34
I_{max} 95% C.I.	-1.53 – 18.53	-19.01 – 33.66	-67.95 – 80.63

(b)

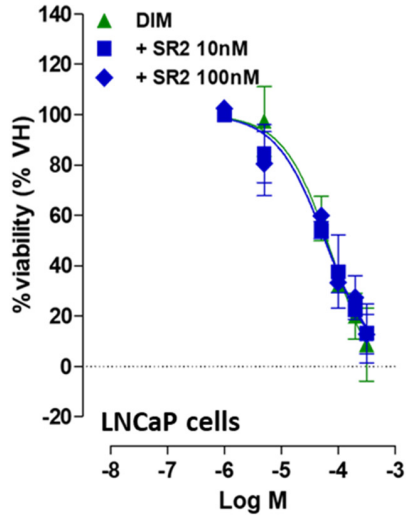

Compound	3′-3′-diindolymethane (DIM)	+ SR144528 (SR2), 10nM	+ SR144528 (SR2), 100nM
IC_{50} (μM)	84.97	59.60	60.90
IC_{50} 95% C.I. (μM)	25.83 – 279.5	24.87 – 142.9	25.53 – 141.4
pIC_{50}	4.071	4.225	4.221
pIC_{50} 95% C.I.	4.588 – 3.554	4.604 – 3.845	4.593 – 3.850
I_{max}	-16.63	-1.41	-0.33
I_{max} 95% C.I.	-65.61 – 32.35	-27.83 – 25.00	-26.12 – 25.46

Figure 3. Effects of DIM and different concentrations of the CB_2 receptor antagonist SR2 on cell viability in PC3 cells (**a**) and LNCaP cells (**b**). Each data point is the mean percentage value ± S.E.M ($n = 7$). IC_{50}, pIC_{50} and I_{max} values and 95% confidence intervals are shown in the table. ** $p < 0.01$ (paired Student's *t*-test).

(a)

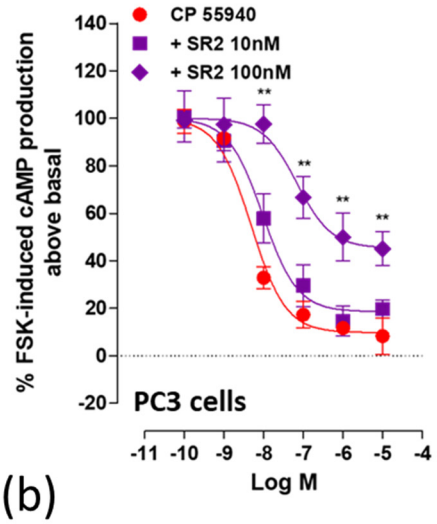

Compound	CP 55,940 (CP)	+ SR144528 (SR2), 10nM	+ SR144528 (SR2), 100nM
IC_{50} (nM)	4.85	9.52	69.36
IC_{50} 95% C.I. (nM)	2.86 – 8.23	4.37 – 20.73	17.91 – 268.5
pIC_{50}	8.314	8.021	6.907
pIC_{50} 95% C.I.	8.543 – 8.805	8.360 – 7.683	7.747 – 6.571
I_{max}	9.74	18.59	45.35
I_{max} 95% C.I.	2.85 – 16.63	8.82 – 28.35	31.59 – 59.10

(b)

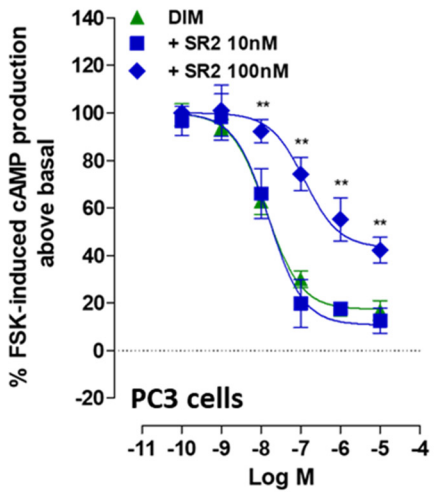

Compound	3′-3′-diindolymethane (DIM)	+ SR144528 (SR2), 10nM	+ SR144528 (SR2), 100nM
IC_{50} (nM)	13.49	15.75	124.9
IC_{50} 95% C.I. (nM)	8.53 – 21.34	5.31 – 46.68	26.07 – 598.7
pIC_{50}	7.870	7.803	7.047
pIC_{50} 95% C.I.	8.069 – 7.671	8.275 – 7.331	7.584 – 6.223
I_{max}	17.36	10.79	43.26
I_{max} 95% C.I.	12.93 – 21.79	-3.74 – 25.32	29.07 – 57.54

Figure 4. Effects of CP 55,940 (**a**) and DIM (**b**) on FSK-induced cAMP production in PC3 cells. The effects of different concentrations of the CB_2 receptor antagonist SR2 in presence of CP 55,940 (**a**) or DIM (**b**) are also shown. Each data point is the mean percentage value ± S.E.M. (n = 10). IC_{50}, pIC_{50} and I_{max} values and 95% confidence intervals are shown in the tables. ** $p < 0.01$ (paired Student's t-test).

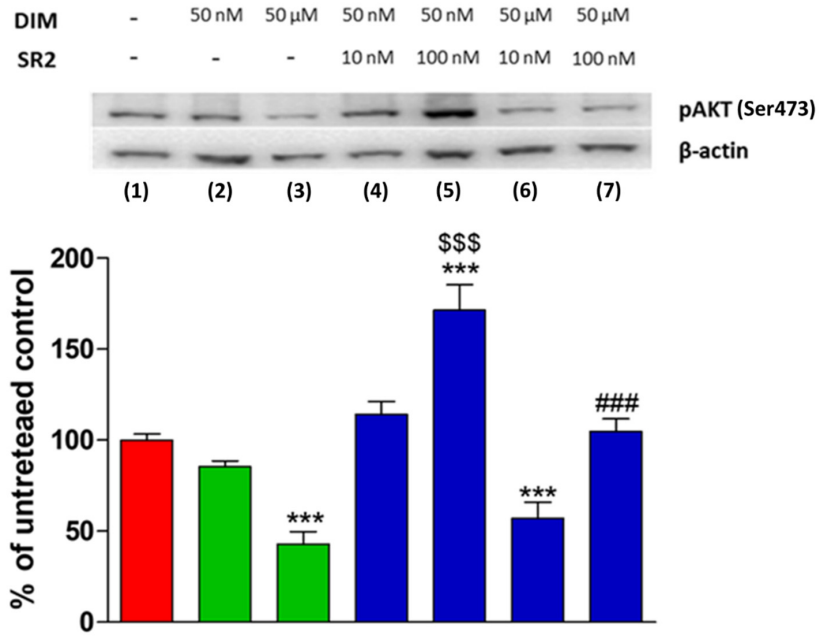

Figure 5. Western blot analysis of phosphor-AKT (Ser473) levels in PC3 cells. The effects of different concentrations of DIM alone and in the presence of different concentrations of the CB_2 receptor antagonist SR2 are shown. Levels are normalized to actin internal loading control and expressed as a percentage compared to untreated control cells. Each data point is the mean percentage value ± S.E.M. (n = 3). *** $p < 0.001$ vs. CTRL (1), $$$ $p < 0.001$ vs. DIM 50 nM (2), ### $p < 0.001$ vs. DIM 50 µM (3). (one-way ANOVA analysis of variance with Tukey's post hoc analysis).

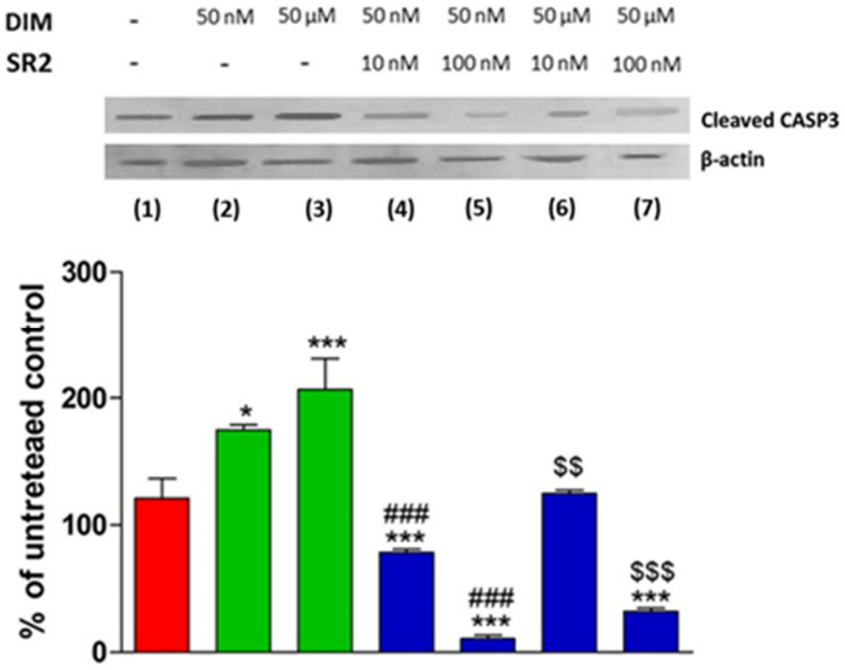

Figure 6. Western blot analysis of cleaved caspase 3 (CASP-3) levels in PC3 cells. The effects of different concentrations of DIM alone and in the presence of different concentrations of the CB_2 receptor antagonist SR2 are shown. Levels are normalized to actin internal loading control and expressed as a percentage compared to untreated control cells. Each data point is the mean percentage value ± S.E.M. (n = 3). * $p < 0.05$ vs. CTRL (1), *** $p < 0.001$ vs. CTRL (1), $$ $p < 0.05$ vs. 50 µM (3), $$$ $p < 0.001$ vs. 50 µM (3), ### $p < 0.001$ vs. 50 nM DIM (2). (one-way ANOVA analysis of variance with Tukey's post hoc analysis).

3. Discussion

The experimental results obtained in our study have clearly demonstrated that the pharmacological effect of DIM was mediated by CB_2 receptors as shown by [^{35}S]GTPγS assay in PC3 and, to a lesser extent, in LNCap cells.

Given the robust effect in PC3 cells, the CB_2 receptor-mediated effect of DIM was further investigated in this cell line. In the cAMP assay experiments, DIM inhibited FSK-induced cAMP production, inhibited pAKT and enhanced cleavage of CASP-3, all of which were robustly antagonized by the CB_2 receptor antagonist.

To our knowledge, there are very few previous studies that describe the ability of DIM to interact with CB_2 cannabinoid receptors, and these used stable CB_2 receptor-transfected cellular models. Thus, this may be the first study to describe the effects in cells endogenously expressing this receptor and the associated signaling pathways. Specifically, a study conducted in 2009 by Yin et al. [22] showed that DIM was only able to partially activate CB_2 receptors when tested in a β-arrestin assay. However, our data in cancer cells in both the [^{35}S]GTPγS and cAMP assays, clearly indicate DIM actually displays full agonist activity, similar to the well-known full CB_1/CB_2 receptor agonist CP 55,940.

The difference in CB_2 receptor properties between the two studies is likely due to the different cellular models (recombinant vs. naturally expressing cell lines) used, although it may also reflect the different assays used to characterize the pharmacological response of the CB_2 receptor to DIM. Whatever the reason, our findings suggest that for the pharmacological characterization of potential CB_2 receptor ligands, systems naturally expressing the receptor represent a more reliable model than recombinant ones when compared to in vivo models [32]. As mentioned above, when tested in both cell lines, DIM behaved as a full CB_2 receptor agonist and, at least in PC3 cells, the compound was also able to induce apoptosis through a significant reduction of the pAKT level. The latter is important since pAKT is a key kinase in multiple cellular pathways involved in oncogenic and proliferative functions that can regulate androgen receptor levels in prostate cancer cells [34].

The main factors influencing the growth and progression of prostate cancer are the androgen receptor and the PI3K/AKT pathway. Our observations, therefore, confirm previous studies showing that the activation of the CB_2 receptor was responsible for AKT protein kinase dephosphorylation in addition to the inhibition of the phosphatidylinositol-3-kinase (PI3K)-AKT pathway [35,36], but importantly, it shows that DIM induces the same effects. The glycogen synthase kinase 3 (GSK-3) and other targets are regulated by AKT phosphorylation increased by the phosphatase and tensin homolog (PTEN) tumor suppressor gene inactivation [37]. PTEN has been reported to be lost or mutated in most advanced prostate cancer cases [38] and there are numerous inhibitors in development that target various PI3K cascade nodes, including PI3K, AKT, mTOR [34]. The effect of DIM on PTEN/PI3K-AKT signaling has been reported in other cancer models [39] and our results suggest it invokes the same inhibitory activity in PC3 cells through CB_2 receptors. On the other hand, PI3K or AKT inhibition might not be enough to significantly reduce tumor size in prostate cancer, and repression of the AR axis is also necessary for maximum effectiveness [37]. In fact, several investigations showed that PI3K and AR signaling interact [40,41]. This may explain the lack of efficacy in LNCaP cell lines, which are thought to be androgen-dependent, requiring androgens for growth. In contrast, PC3 cell lines are thought to be androgen-independent, not requiring or affecting androgen for growth [42]. It is likely that LNCaP cells with a functioning androgen pathway prevent DIM from activating CB2. In LNCaP cells, the DIM-induced inhibition of cell viability was not antagonized by the CB_2 receptors antagonist, suggesting the possible involvement of other non-cannabinoid receptors in the mechanism. In fact, in LNCaP cells, DIM can inhibit cancer cell proliferation through different and overlapping mechanisms [43,44] and some cannabinoid ligands have been reported to induce apoptosis through a combination of cannabinoid receptor-independent cellular and molecular mechanisms [45]. Our results, obtained by stimulating LNCaP with DIM, show only a weak effect on cell proliferation

which may be ascribed to a non-specific mechanism or to a lower expression of CB_2 receptors in this cell line [45].

In PC3 cells, activation of the CB_2 receptor can elicit an antiproliferative effect by promoting an increase in ceramide levels [46]. Ceramide generation occurs from sphingomyelin hydrolysis, with cannabinoids having a stimulatory effect in the process [47]. Indeed, increasing ceramide levels can inhibit the AKT-mammalian target of the rapamycin (mTOR) pathway and activate the initiation factors involved in autophagy regulation and endoplasmic reticulum (ER) stress response [27]. Also, increasing levels of ceramide due to ER stress enhancement can trigger the activation of the caspase cascade, leading to apoptosis as well [27]. As cysteine proteases, caspases are formed constitutively in the cells and are normally present as inactive proenzymes [48]. In this context, our results have shown that treating PC3 cells with DIM caused a significantly increased level of the active pro-apoptotic caspase-3 (CASP-3) kinase, confirming the ability of the compound to induce apoptosis in this human prostate cancer cell line [48].

The CB_2 receptor-mediated AKT dephosphorylation in PC3 cells after DIM administration may suggest a different signaling pathway is involved, one not involving the activation of PI3K, a kinase normally activated by $G_{\beta\gamma}$ subunits upon CB_2 receptor stimulation [49]. Indeed, the PI3K pathway is directly responsible for AKT activation and provides an intrinsic bypass mechanism able to enhance both the survival and proliferation of prostate cancer cells lacking AR signaling, making these cells resistant to androgen therapy [50]. Thus, the inhibitory role of CB_2 receptors on AKT, possibly through a mechanism independent of PI3K, may represent promising and beneficial effects of DIM that are worth further investigation, considering the lack of demonstrable efficacy in clinical studies where direct PI3K inhibitor drugs were tested. [50].

Our data suggest that PC3 cells exhibit a constitutively active tone by the endocannabinoids on CB_2 receptors which modulates the AKT pathway. This is demonstrated as the AKT phosphorylation increased significantly above the basal levels when the effect of DIM was antagonized with the highest dose of CB_2 receptor antagonist [28].

As mentioned above, in human prostate cancer cells, antiproliferative and apoptotic effects can also be mediated by ceramide accumulation and these compounds have been suggested as possible mediators of cannabinoid action, and more specifically, of the endogenous cannabinoid anandamide [27]. Consistent with this, altered levels of intracellular ceramide have been found in both LNCaP and PC3 cells [51].

4. Materials and Methods

4.1. Culturing and Treatment of Cells

Human prostate cancer cell lines, LNCaP and PC3, were obtained from the European Collection of Animal Cell Cultures. These were cultured in RPMI 1640 medium (Merck Life Science Ltd, Gillingham, UK) containing 10% (*vol:vol*) fetal bovine serum and 1% (*vol:vol*) Penicillin–Streptomycin Solution (10,000 U/mL penicillin and 10 mg/mL streptomycin in 0.9% sodium chloride (Merck Life Science Ltd., Gillingham, UK).

4.2. Biochemical Reagents

CP 55,940 (Merck Life Science Ltd., Gillingham, UK), CB_1 and CB_2 receptors agonist, CB_1- and CB_2- selective inverse agonists, SR 141716 (SR1) and SR 144528 (SR2) (Bio-Techne Ltd., Abingdon, UK), were dissolved in dimethyl sulfoxide (DMSO) and all stored at 10 mM stock solutions (−20 °C).

Appropriate concentrations were freshly prepared from stock solution using a culture medium. DMSO and ethanol diluent controls were also in. For binding experiments, [^{35}S] guanosine 5′-O-[gamma-thio] triphosphate (GTPγS) (1250 Ci/mmol) was obtained from PerkinElmer Life Sciences (Stapeley, Nantwich, UK), GTPγS and adenosine deaminase from Roche Diagnostic (Merck Life Science Ltd., Gillingham, UK) and guanosine diphosphate (GDP) and phenylmethylsulfonyl fluoride (PMSF) from Merck Life Science Ltd., Gillingham, UK. All cells and chemicals were handled using the appropriate personal

protective equipment. The DIM concentrations used in this study were chosen according to pharmacokinetic studies in animals and previous studies in prostate cancer cell lines [52].

4.3. Membrane Preparation

Binding assays with [^{35}S]GTPγS were performed with PC3 or LNCaP cell membranes [53,54]. Both PC3 and LNCaP cells were removed from flasks by scraping and then frozen as a pellet at −20 °C until required [55]. Before use in a radioligand-binding assay, cells were defrosted, diluted in Tris buffer (50 mM Tris–HCl, 50 mM Tris-Base) and homogenized. Protein assays were performed using a Bio-Rad Dc kit (Bio-Rad©, Watford, UK).

4.4. [^{35}S]GTPγS-Binding Assays

The measurement of ligand-stimulated [^{35}S]GTPγS binding to cannabinoid CB_1 or CB_2 receptors was adapted from methods described previously [55,56]. The assays were carried out with GTPγS-binding buffer (50 mM Tris–HCl, 50 mM Tris-Base, 5 mM $MgCl_2$, 1 mM ethylenediaminetetraacetic acid, 100 mM NaCl, 1 mM dithiothreitol and 0.1% bovine serum albumin) in the presence of [^{35}S]GTPγS and GDP, in a final volume of 500 µL. Binding was initiated by the addition of [^{35}S]GTPγS to the wells. Non-specific binding was measured in the presence of 30 µM GTPγS. The drugs were incubated in the assay for 60 min at 30 °C. The reaction was terminated by a rapid vacuum filtration method using Tris-binding buffer, as described previously [32], and the radioactivity was quantified by liquid scintillation spectrometry. In all the [^{35}S]GTPγS-binding assays, we used 0.1 nM [^{35}S]GTPγS, 30 µM GDP and a protein concentration of 40 µg per well for PC3 and LNCaP cell membranes. Compounds were stored at −20 °C in DMSO.

4.5. Cyclic AMP Assay

The assays were performed using the HitHunter® cAMP assay kit (Eurofins DiscoverX Products, Celle-L'Evescault, France) according to the vendor's protocol and previous studies [32,57]. Briefly, cells were detached using cell dissociation buffer, counted and seeded at 2×10^4 cells per well in 100 mL of complete medium onto white 96-well plates and incubated at 37 °C and 5% CO_2 for approximately 24 h before running the experiment. The assays and the drug dilutions were performed in a 1:1 mixture of DMEM and Ham's F12 medium without phenol red, containing 10 mM of rolipram and forskolin (FSK; 7b-acetoxy-8,13-epoxy-1a,6b,9 atrihydroxylabd-14-en-11-one). Before running the assay, the medium was discarded, and cells were washed with D-MEM/F-12 medium. Then, cells were treated with the assigned drugs (30 µL per well) and incubated for 30 min at 37 °C and 5% CO_2. Finally, cAMP standards and the appropriate mixture of kit components were added (as described by the manufacturer, Eurofins DiscoverX Products, Celle-L'Evescault, France). Plates were incubated overnight at room temperature in the dark. Chemiluminescent signals were detected on a Synergy HT Multi-Mode Microplate Reader (ThermoFisher Scientific, Loughborough, UK).

4.6. Cell Viability Assay

A standard 3-(4,-5-dimethylthiazol-2-yl)-2,-5-diphenyl tetrazolium bromide (MTT) dye reduction assay was used to assess compounds. Briefly, cells were plated in a flat-bottomed 96-well plate at seeding densities of 6×10^3 cells per well for LNCaP cells and 5×10^3 cells per well for PC3 cells. Cells were treated the following day with the appropriate agents for 24 h. Following the incubation period, the MTT solution (5 mg/mL in phosphate-buffered saline) was added and incubated for 4 h. The contents of the wells were removed and replaced with 200 µL DMSO to dissolve the MTT formazan crystals. The plates were immediately read at 570 nm in a multi-well plate reader (DynaTech MR5000; Dynex Technologies Ltd., Chantilly, VA, USA).

4.7. Protein Analysis

Cells were homogenized in lysis buffer [20 mM Tris, 0.25 M sucrose, 10 mM ethyleneglycol-bis(aminoethylether)-tetraacetic acid, 2 mM ethylenediaminetetraacetic acid, 1 mM sodium orthovanadate, 25 mM sodium β-glycerophosphate and 50 mM sodium fluoride; pH 7.5]. Prior to use, 0.1% (*vol:vol*), protease Inhibitor Cocktail (Merck Life Science Ltd, Gillingham, UK) was added. A total of 20 µg of protein was electrophoresed through a precast 16% polyacrylamide gel (Thermo Fisher, Oxford, UK) for 2 h and the separated proteins were transferred to nitrocellulose membranes (Bio-Rad, UK), then blocked with 5% (*wt:vol*) skimmed milk in Tris-buffered saline with 0.1% (*vol:vol*) Tween 20 (TBST solution) at room temperature and incubated with 1:200 dilution of anti-pAKT (Ser473) antibody (Merck Life Science Limited, Watford, Hertfordshire UK) or 1:200 cleaved-CASP-3 antibody (Insight Biotechnology, UK) at 4 °C overnight. β-Actin (1:20,000) was used as an internal loading control to normalize between lanes during densitometry. The appropriate secondary antibody for pAKT (anti-mouse), cleaved-CASP-3 (anti-mouse) was used at a concentration of 1:5000 (Insight Biotechnology Ltd, Wembley, Middlesex, UK) and incubated at room temperature for 1 h. Proteins were visualized using ECL plus™ chemiluminescent detection kit (Abcam plc, Trumpington, Cambridge, UK), according to the manufacturer's instructions, and a Fluor S phosphorimager (Bio-Rad©, Watford, UK). The experiments were performed with proteins isolated from three independent extractions.

4.8. Data Analysis

Values for half of the maximal effective concentration required to elicit a response (EC_{50}), or for the half maximal inhibitory concentration (IC_{50}) required to inhibit a response, as well as for maximal effect (E_{max}), standard error of the mean (S.E.M.) and 95% confidence limits of EC_{50} and IC_{50}, have been calculated by nonlinear regression analysis using the equation for a sigmoid concentration–response curve (GraphPad Prism v5.0, San Diego, CA, USA). Paired Student's *t*-test or one-way ANOVA analysis of variance (with Tukey's post hoc analysis) was used where appropriate for cell viability and western blotting data. A value of $p < 0.05$ was taken as being significant.

5. Conclusions

Bringing together our results, we can conclude that DIM is a CB_2 receptor ligand with a potential anti-prostate cancer effect, and differing from classical cannabinoids, is without any psychotropic activity. In particular, DIM can induce a significant anti-apoptotic activity in the androgen-independent human prostate cancer cell line PC3, a cellular model that mimics prostatic small cell neuroendocrine carcinoma (SCNC), an extremely aggressive form of prostate cancer resistant to standard hormonal therapy [58,59]. According to reports, unlike LNCaP cells, PC3 cells do not express AR and their proliferation is androgen-independent, much like SCNC [58]. A more consistent body of evidence is required to confirm our findings and better understand the biological activity of DIM. The promising results obtained in this study represent a step forward in the understanding of the mechanism(s) underlying the DIM anticancer effect and encourage further exploration into the beneficial effect of this compound for the treatment of those forms of prostate cancer insensitive to the androgen treatment.

Based on our results, we have estimated that the concentrations at which DIM is showing an effect on cell viability could be obtained in vivo with an equivalent daily intake of about 60 mg of the compound. However, such daily intakes cannot be achieved by the ingestion of *Brassica* vegetables alone, therefore, administration in form of supplements may be required [60].

Author Contributions: Conceptualization, P.T. and P.M.; methodology, P.T., I.B., R.G.P. and P.M.; software, P.T., I.B., R.G.P. and P.M.; validation, P.T., R.G.P. and P.M.; formal analysis, P.T. and P.M.; investigation, P.T., I.B., G.S.B., R.G.P. and P.M.; resources, R.G.P., P.M. and I.B.; data curation, P.T. and P.M.; writing—original draft preparation, P.T., G.S.B. and P.M.; writing—review and editing, P.T., I.B., G.S.B., R.G.P. and P.M.; visualization, P.T., G.S.B. and P.M.; supervision, P.T.; project administration, P.T. and P.M.; funding acquisition, R.G.P., P.M. and I.B. All authors have read and agreed to the published version of the manuscript.

Funding: This research was funded by Friends of Anchor (charity no SC025332, Aberdeen, UK), grant number RGB4100, awarded to Prof R.G. Pertwee (R.P.), Pietro Marini (P.M.) and I. Brown (I.B.).

Informed Consent Statement: Not applicable.

Data Availability Statement: Data is contained within the article.

Acknowledgments: The authors wish to thank Iain McEwan for his helpful comments during the preparation of this work.

Conflicts of Interest: The authors declare no conflict of interest.

References

1. Tucci, P.; Bove, M.; Sikora, V.; Dimonte, S.; Morgese, M.G.; Schiavone, S.; Di Cesare Mannelli, L.; Ghelardini, C.; Trabace, L. Glucoraphanin Triggers Rapid Antidepressant Responses in a Rat Model of Beta Amyloid-Induced Depressive-like Behaviour. *Pharmaceuticals* **2022**, *15*, 1054. [CrossRef]
2. Ibrahim, N.; Allart-Simon, I.; De Nicola, G.R.; Iori, R.; Renault, J.-H.; Rollin, P.; Nuzillard, J.-M. Advanced NMR-Based Structural Investigation of Glucosinolates and Desulfoglucosinolates. *J. Nat. Prod.* **2018**, *81*, 323–334. [CrossRef]
3. Fuentes, F.; Paredes-Gonzalez, X.; Kong, A.-N.T. Dietary Glucosinolates Sulforaphane, Phenethyl Isothiocyanate, Indole-3-Carbinol/3,3′-Diindolylmethane: Anti-Oxidative Stress/Inflammation, Nrf2, Epigenetics/Epigenomics and In Vivo Cancer Chemopreventive Efficacy. *Curr. Pharmacol. Rep.* **2015**, *1*, 179–196. [CrossRef] [PubMed]
4. Armeli, F.; Bonucci, A.; Maggi, E.; Pinto, A.; Businaro, R. Mediterranean Diet and Neurodegenerative Diseases: The Neglected Role of Nutrition in the Modulation of the Endocannabinoid System. *Biomolecules* **2021**, *11*, 790. [CrossRef]
5. Vang, O. Chemopreventive Potential of Compounds in Cruciferous Vegetables. In *Carcinogenic and Anticarcinogenic Food Components*; Baer-Dubowska, W., Bartoszek, A., Malejka-Giganti, D., Eds.; CRC Press: Boca Raton, FL, USA, 2005; pp. 303–328. ISBN 978-0-8493-2096-5.
6. Licznerska, B.; Baer-Dubowska, W. Indole-3-Carbinol and Its Role in Chronic Diseases. In *Anti-inflammatory Nutraceuticals and Chronic Diseases*; Gupta, S.C., Prasad, S., Aggarwal, B.B., Eds.; Advances in Experimental Medicine and Biology; Springer International Publishing: Cham, Switzerland, 2016; Volume 928, pp. 131–154. ISBN 978-3-319-41332-7.
7. Anderton, M.J.; Manson, M.M.; Verschoyle, R.D.; Gescher, A.; Lamb, J.H.; Farmer, P.B.; Steward, W.P.; Williams, M.L. Pharmacokinetics and Tissue Disposition of Indole-3-Carbinol and Its Acid Condensation Products after Oral Administration to Mice. *Clin. Cancer Res.* **2004**, *10*, 5233–5241. [CrossRef]
8. Anderton, M.J.; Manson, M.M.; Verschoyle, R.; Gescher, A.; Steward, W.P.; Williams, M.L.; Mager, D.E. Physiological Modeling of Formulated and Crystalline 3,3′-Diindolylmethane Pharmacokinetics Following Oral Administration in Mice. *Drug Metab. Dispos.* **2004**, *32*, 632–638. [CrossRef] [PubMed]
9. Fujioka, N.; Ainslie-Waldman, C.E.; Upadhyaya, P.; Carmella, S.G.; Fritz, V.A.; Rohwer, C.; Fan, Y.; Rauch, D.; Le, C.; Hatsukami, D.K.; et al. Urinary 3,3′-Diindolylmethane: A Biomarker of Glucobrassicin Exposure and Indole-3-Carbinol Uptake in Humans. *Cancer Epidemiol Biomarkers Prev* **2014**, *23*, 282–287. [CrossRef] [PubMed]
10. Reed, G.A.; Arneson, D.W.; Putnam, W.C.; Smith, H.J.; Gray, J.C.; Sullivan, D.K.; Mayo, M.S.; Crowell, J.A.; Hurwitz, A. Single-Dose and Multiple-Dose Administration of Indole-3-Carbinol to Women: Pharmacokinetics Based on 3,3′-Diindolylmethane. *Cancer Epidemiol. Biomarkers Prev.* **2006**, *15*, 2477–2481. [CrossRef]
11. Zhang, W.W.; Feng, Z.; Narod, S.A. Multiple Therapeutic and Preventive Effects of 3,3′-Diindolylmethane on Cancers Including Prostate Cancer and High Grade Prostatic Intraepithelial Neoplasia. *J. Biomed. Res.* **2014**, *28*, 339–348. [CrossRef]
12. Wang, S.; Cheng, L.; Liu, Y.; Wang, J.; Jiang, W. Indole-3-Carbinol (I3C) and Its Major Derivatives: Their Pharmacokinetics and Important Roles in Hepatic Protection. *Curr. Drug Metab.* **2016**, *17*, 401–409. [CrossRef]
13. Li, Y.; Kong, D.; Ahmad, A.; Bao, B.; Sarkar, F.H. Antioxidant Function of Isoflavone and 3,3′-Diindolylmethane: Are They Important for Cancer Prevention and Therapy? *Antioxid. Redox Signal.* **2013**, *19*, 139–150. [CrossRef]
14. Hayes, J.D.; Kelleher, M.O.; Eggleston, I.M. The Cancer Chemopreventive Actions of Phytochemicals Derived from Glucosinolates. *Eur. J. Nutr.* **2008**, *47* (Suppl. 2), 73–88. [CrossRef] [PubMed]
15. Jemal, A.; Bray, F.; Center, M.M.; Ferlay, J.; Ward, E.; Forman, D. Global Cancer Statistics. *CA Cancer J. Clin.* **2011**, *61*, 69–90. [CrossRef]
16. Tannock, I.F. Improving Treatment for Advanced Prostate Cancer. *N. Engl. J. Med.* **2019**, *381*, 176–177. [CrossRef]

17. Le, H.T.; Schaldach, C.M.; Firestone, G.L.; Bjeldanes, L.F. Plant-Derived 3,3′-Diindolylmethane Is a Strong Androgen Antagonist in Human Prostate Cancer Cells. *J. Biol. Chem.* **2003**, *278*, 21136–21145. [CrossRef]
18. Chen, I.; Safe, S.; Bjeldanes, L. Indole-3-Carbinol and Diindolylmethane as Aryl Hydrocarbon (Ah) Receptor Agonists and Antagonists in T47D Human Breast Cancer Cells. *Biochem. Pharmacol.* **1996**, *51*, 1069–1076. [CrossRef]
19. Chen, I.; McDougal, A.; Wang, F.; Safe, S. Aryl Hydrocarbon Receptor-Mediated Antiestrogenic and Antitumorigenic Activity of Diindolylmethane. *Carcinogenesis* **1998**, *19*, 1631–1639. [CrossRef] [PubMed]
20. Li, Y.; Li, X.; Sarkar, F.H. Gene Expression Profiles of I3C- and DIM-Treated PC3 Human Prostate Cancer Cells Determined by CDNA Microarray Analysis. *J. Nutr.* **2003**, *133*, 1011–1019. [CrossRef] [PubMed]
21. Paltsev, M.; Kiselev, V.; Drukh, V.; Muyzhnek, E.; Kuznetsov, I.; Andrianova, E.; Baranovskiy, P. First Results of the Double-Blind Randomized Placebo-Controlled Multicenter Clinical Trial of DIM-Based Therapy Designed as Personalized Approach to Reverse Prostatic Intraepithelial Neoplasia (PIN). *EPMA J.* **2016**, *7*, 5. [CrossRef]
22. Yin, H.; Chu, A.; Li, W.; Wang, B.; Shelton, F.; Otero, F.; Nguyen, D.G.; Caldwell, J.S.; Chen, Y.A. Lipid G Protein-Coupled Receptor Ligand Identification Using Beta-Arrestin PathHunter Assay. *J. Biol. Chem.* **2009**, *284*, 12328–12338. [CrossRef]
23. Ramer, R.; Schwarz, R.; Hinz, B. Modulation of the Endocannabinoid System as a Potential Anticancer Strategy. *Front. Pharmacol.* **2019**, *10*, 430. [CrossRef] [PubMed]
24. Schmid, P.C.; Wold, L.E.; Krebsbach, R.J.; Berdyshev, E.V.; Schmid, H.H.O. Anandamide and Other N-Acylethanolamines in Human Tumors. *Lipids* **2002**, *37*, 907–912. [CrossRef]
25. Pagano, C.; Navarra, G.; Coppola, L.; Bifulco, M.; Laezza, C. Molecular Mechanism of Cannabinoids in Cancer Progression. *Int. J. Mol. Sci.* **2021**, *22*, 3680. [CrossRef] [PubMed]
26. Díaz-Laviada, I. The Endocannabinoid System in Prostate Cancer. *Nat. Rev. Urol.* **2011**, *8*, 553–561. [CrossRef]
27. Singh, K.; Nassar, N.; Bachari, A.; Schanknecht, E.; Telukutla, S.; Zomer, R.; Piva, T.J.; Mantri, N. The Pathophysiology and the Therapeutic Potential of Cannabinoids in Prostate Cancer. *Cancers* **2021**, *13*, 4107. [CrossRef] [PubMed]
28. Orellana-Serradell, O.; Poblete, C.E.; Sanchez, C.; Castellón, E.A.; Gallegos, I.; Huidobro, C.; Llanos, M.N.; Contreras, H.R. Proapoptotic Effect of Endocannabinoids in Prostate Cancer Cells. *Oncol. Rep.* **2015**, *33*, 1599–1608. [CrossRef]
29. Sampson, N.; Neuwirt, H.; Puhr, M.; Klocker, H.; Eder, I.E. In Vitro Model Systems to Study Androgen Receptor Signaling in Prostate Cancer. *Endocr.-Relat. Cancer* **2013**, *20*, R49–R64. [CrossRef]
30. Brown, I.; Cascio, M.G.; Wahle, K.W.J.; Smoum, R.; Mechoulam, R.; Ross, R.A.; Pertwee, R.G.; Heys, S.D. Cannabinoid Receptor-Dependent and -Independent Anti-Proliferative Effects of Omega-3 Ethanolamides in Androgen Receptor-Positive and -Negative Prostate Cancer Cell Lines. *Carcinogenesis* **2010**, *31*, 1584–1591. [CrossRef]
31. Bolognini, D.; Cascio, M.G.; Parolaro, D.; Pertwee, R.G. AM630 Behaves as a Protean Ligand at the Human Cannabinoid CB2 Receptor. *Br. J. Pharmacol.* **2012**, *165*, 2561–2574. [CrossRef]
32. Marini, P.; Cascio, M.-G.; King, A.; Pertwee, R.G.; Ross, R.A. Characterization of Cannabinoid Receptor Ligands in Tissues Natively Expressing Cannabinoid CB2 Receptors. *Br. J. Pharmacol.* **2013**, *169*, 887–899. [CrossRef]
33. Fong, T.M. Measurement of Inverse Agonism of the Cannabinoid Receptors. In *Methods in Enzymology*; Elsevier: Amsterdam, The Netherlands, 2010; Volume 485, pp. 139–145. ISBN 978-0-12-381296-4.
34. Shorning, B.Y.; Dass, M.S.; Smalley, M.J.; Pearson, H.B. The PI3K-AKT-MTOR Pathway and Prostate Cancer: At the Crossroads of AR, MAPK, and WNT Signaling. *Int. J. Mol. Sci.* **2020**, *21*, 4507. [CrossRef]
35. Wang, J.; Xu, J.; Peng, Y.; Xiao, Y.; Zhu, H.; Ding, Z.-M.; Hua, H. Phosphorylation of Extracellular Signal-Regulated Kinase as a Biomarker for Cannabinoid Receptor 2 Activation. *Heliyon* **2018**, *4*, e00909. [CrossRef] [PubMed]
36. Louka, S.; Neophytou, C.; Constantinou, A. Abstract 4030: Synthetic Cannabinoids AM-251 and AM-1241 Induce Cell Death in Prostate Cancer Cells. *Cancer Res.* **2020**, *80*, 4030. [CrossRef]
37. Marques, R.B.; Aghai, A.; de Ridder, C.M.A.; Stuurman, D.; Hoeben, S.; Boer, A.; Ellston, R.P.; Barry, S.T.; Davies, B.R.; Trapman, J.; et al. High Efficacy of Combination Therapy Using PI3K/AKT Inhibitors with Androgen Deprivation in Prostate Cancer Preclinical Models. *Eur. Urol.* **2015**, *67*, 1177–1185. [CrossRef] [PubMed]
38. Lotan, T.L.; Gurel, B.; Sutcliffe, S.; Esopi, D.; Liu, W.; Xu, J.; Hicks, J.L.; Park, B.H.; Humphreys, E.; Partin, A.W.; et al. PTEN Protein Loss by Immunostaining: Analytic Validation and Prognostic Indicator for a High Risk Surgical Cohort of Prostate Cancer Patients. *Clin. Cancer Res.* **2011**, *17*, 6563–6573. [CrossRef] [PubMed]
39. Wang, X.; Zhao, Y.; Yu, M.; Xu, Y. PTEN/Akt Signaling-Mediated Activation of the Mitochondrial Pathway Contributes to the 3,3′-Diindolylmethane-Mediated Antitumor Effect in Malignant Melanoma Cells. *J. Med. Food* **2020**, *23*, 1248–1258. [CrossRef]
40. Mulholland, D.J.; Tran, L.M.; Li, Y.; Cai, H.; Morim, A.; Wang, S.; Plaisier, S.; Garraway, I.P.; Huang, J.; Graeber, T.G.; et al. Cell Autonomous Role of PTEN in Regulating Castration-Resistant Prostate Cancer Growth. *Cancer Cell* **2011**, *19*, 792–804. [CrossRef]
41. Carver, B.S.; Chapinski, C.; Wongvipat, J.; Hieronymus, H.; Chen, Y.; Chandarlapaty, S.; Arora, V.K.; Le, C.; Koutcher, J.; Scher, H.; et al. Reciprocal Feedback Regulation of PI3K and Androgen Receptor Signaling in PTEN-Deficient Prostate Cancer. *Cancer Cell* **2011**, *19*, 575–586. [CrossRef]
42. Sailer, V.; von Amsberg, G.; Duensing, S.; Kirfel, J.; Lieb, V.; Metzger, E.; Offermann, A.; Pantel, K.; Schuele, R.; Taubert, H.; et al. Experimental in Vitro, Ex Vivo and in Vivo Models in Prostate Cancer Research. *Nat. Rev. Urol.* 2022; *Online ahead of print*. [CrossRef]
43. Savino, J.A.; Evans, J.F.; Rabinowitz, D.; Auborn, K.J.; Carter, T.H. Multiple, Disparate Roles for Calcium Signaling in Apoptosis of Human Prostate and Cervical Cancer Cells Exposed to Diindolylmethane. *Mol. Cancer Ther.* **2006**, *5*, 556–563. [CrossRef]

44. Chen, D.; Banerjee, S.; Cui, Q.C.; Kong, D.; Sarkar, F.H.; Dou, Q.P. Activation of AMP-Activated Protein Kinase by 3,3′-Diindolylmethane (DIM) Is Associated with Human Prostate Cancer Cell Death In Vitro and In Vivo. *PLoS ONE* **2012**, *7*, e47186. [CrossRef]
45. Sarfaraz, S.; Afaq, F.; Adhami, V.M.; Mukhtar, H. Cannabinoid Receptor as a Novel Target for the Treatment of Prostate Cancer. *Cancer Res.* **2005**, *65*, 1635–1641. [CrossRef] [PubMed]
46. Olea-Herrero, N.; Vara, D.; Malagarie-Cazenave, S.; Díaz-Laviada, I. Inhibition of Human Tumour Prostate PC-3 Cell Growth by Cannabinoids R(+)-Methanandamide and JWH-015: Involvement of CB2. *Br. J. Cancer* **2009**, *101*, 940–950. [CrossRef]
47. Guzmán, M.; Galve-Roperh, I.; Sánchez, C. Ceramide: A New Second Messenger of Cannabinoid Action. *Trends Pharmacol. Sci.* **2001**, *22*, 19–22. [CrossRef]
48. Nachshon-Kedmi, M.; Yannai, S.; Fares, F.A. Induction of Apoptosis in Human Prostate Cancer Cell Line, PC3, by 3,3′-Diindolylmethane through the Mitochondrial Pathway. *Br. J. Cancer* **2004**, *91*, 1358–1363. [CrossRef]
49. Zhang, R.; Xie, X. Tools for GPCR Drug Discovery. *Acta Pharmacol. Sin.* **2012**, *33*, 372–384. [CrossRef]
50. Park, S.; Kim, Y.S.; Kim, D.Y.; So, I.; Jeon, J.-H. PI3K Pathway in Prostate Cancer: All Resistant Roads Lead to PI3K. *Biochim. Biophys. Acta (BBA) Rev. Cancer* **2018**, *1870*, 198–206. [CrossRef] [PubMed]
51. Trapika, I.G.M.G.S.C.; Liu, X.T.; Chung, L.H.; Lai, F.; Xie, C.; Zhao, Y.; Cui, S.; Chen, J.; Tran, C.; Wang, Q.; et al. Ceramide Regulates Anti-Tumor Mechanisms of Erianin in Androgen-Sensitive and Castration-Resistant Prostate Cancers. *Front. Oncol.* **2021**, *11*, 738078. [CrossRef]
52. Patel, A.R.; Spencer, S.D.; Chougule, M.B.; Safe, S.; Singh, M. Pharmacokinetic Evaluation and In Vitro–In Vivo Correlation (IVIVC) of Novel Methylene-Substituted 3,3′ Diindolylmethane (DIM). *Eur. J. Pharm. Sci.* **2012**, *46*, 8–16. [CrossRef] [PubMed]
53. Ross, R.A.; Brockie, H.C.; Stevenson, L.A.; Murphy, V.L.; Templeton, F.; Makriyannis, A.; Pertwee, R.G. Agonist-Inverse Agonist Characterization at CB1 and CB2 Cannabinoid Receptors of L759633, L759656, and AM630. *Br. J. Pharmacol.* **1999**, *126*, 665–672. [CrossRef] [PubMed]
54. Thomas, A.; Ross, R.A.; Saha, B.; Mahadevan, A.; Razdan, R.K.; Pertwee, R.G. 6″-Azidohex-2″-Yne-Cannabidiol: A Potential Neutral, Competitive Cannabinoid CB1 Receptor Antagonist. *Eur. J. Pharmacol.* **2004**, *487*, 213–221. [CrossRef] [PubMed]
55. Kurkinen, K.M.; Koistinaho, J.; Laitinen, J.T. [Gamma-35S]GTP Autoradiography Allows Region-Specific Detection of Muscarinic Receptor-Dependent G-Protein Activation in the Chick Optic Tectum. *Brain Res.* **1997**, *769*, 21–28. [CrossRef] [PubMed]
56. Breivogel, C.S.; Griffin, G.; Di Marzo, V.; Martin, B.R. Evidence for a New G Protein-Coupled Cannabinoid Receptor in Mouse Brain. *Mol. Pharmacol.* **2001**, *60*, 155–163. [CrossRef]
57. Marini, P.; Cascio, M.G.; Pertwee, R.G. The Cyclic AMP Assay Using Human Cannabinoid CB2 Receptor-Transfected Cells. *Methods Mol. Biol.* **2016**, *1412*, 85–93. [CrossRef] [PubMed]
58. Tai, S.; Sun, Y.; Squires, J.M.; Zhang, H.; Oh, W.K.; Liang, C.-Z.; Huang, J. PC3 Is a Cell Line Characteristic of Prostatic Small Cell Carcinoma. *Prostate* **2011**, *71*, 1668–1679. [CrossRef]
59. Formaggio, N.; Rubin, M.A.; Theurillat, J.-P. Loss and Revival of Androgen Receptor Signaling in Advanced Prostate Cancer. *Oncogene* **2021**, *40*, 1205–1216. [CrossRef]
60. Chang, X.; Firestone, G.L.; Bjeldanes, L.F. Inhibition of Growth Factor-Induced Ras Signaling in Vascular Endothelial Cells and Angiogenesis by 3,3′-Diindolylmethane. *Carcinogenesis* **2006**, *27*, 541–550. [CrossRef]